

A Heat Pump for Space Applications

H.J. van Gerner¹, G. van Donk², A. Pauw³, and J. van Es⁴
National Aerospace Laboratory NLR, Amsterdam, The Netherlands

and

S. Lapensée⁵
European Space Agency, ESA/ESTEC, Noordwijk ZH, The Netherlands

In commercial communication satellites, waste heat (5-10kW) has to be radiated into space by radiators. These radiators determine the size of the spacecraft, and a further increase in radiator size (and therefore spacecraft size) to increase the heat rejection capacity is not practical. A heat pump can be used to raise the radiator temperature above the temperature of the equipment, which results in a higher heat rejecting capacity without increasing the size of the radiators. A heat pump also provides the opportunity to use East/West radiators, which become almost as effective as North/South radiators when the temperature is elevated to 100°C. The heat pump works with the vapour compression cycle and requires a compressor. However, commercially available compressors have a high mass (40 kg for 10kW cooling capacity), cause excessive vibrations, and are intended for much lower temperatures (maximum 65°C) than what is required for the space heat pump application (100°C). Dedicated aerospace compressors have been developed with a lower mass (19 kg) and for higher temperatures, but these compressors have a lower efficiency. For this reason, an electrically-driven, high-speed (200,000 RPM), centrifugal compressor system has been developed in a project funded by the European Space Agency (ESA). This novel 3-stage compressor system has a mass of just 2 kg and a higher efficiency than existing aerospace compressors. The compressor system has been incorporated in a heat pump demonstrator, which uses isopentane (R601a) as refrigerant. Due to the exposure of isopentane to radiation in a space application, other substances will form. However, a literature study shows that the amounts of the formed substances are so small, that no significant influence on the performance of the heat pump is expected. Tests were carried out with the heat pump, and at the target setting (saturation temperature of 45°C at the evaporator, 100°C at the condenser, and a payload heat input of 5 kW), the measured COP is 2.3, which is higher than the original requirement of 2.

Nomenclature and Abbreviations

COP	=	Coefficient of Performance
ESA	=	European Space Agency
h	=	Specific enthalpy (J/kg)
P_{cool}	=	Cooling power of the heat pump (J/s)
$P_{\text{cooling water}}$	=	Amount of power that is transported away from the compressor by the cooling water (J/s)
RPM	=	Round Per Minute
t	=	facesheet thickness (m)
$W_{\text{compressor}}$	=	Power delivered to the fluid by the compressor (J/s)

¹ R&D Engineer, Space Systems, Henk.Jan.van.Gerner@nlr.nl, +31 88 511 4628.

² Senior Application Engineer, Space Systems, Gerrit.van.Donk@nlr.nl, +31 88 511 4273.

³ Senior Application Engineer, Space Systems, Aswin.Pauw@nlr.nl, +31 88 511 4268.

⁴ Senior R&D Manager, Space Systems, Johannes.van.Es@nlr.nl, +31 88 511 4230.

⁵ Thermal engineer, Thermal Division (TEC-MT), Stephane.Lapensee@esa.int@esa.int, +31 71 565 8733

I. Introduction

In commercial communication satellites, waste heat has to be radiated into space by radiators. These radiators largely determine the size of the spacecraft, and a further increase in radiator size (and therefore spacecraft size) to increase the heat rejection capacity is not practical. In traditional methods for spacecraft thermal control, the radiator temperature must be lower than the payload temperature. A heat pump can be used to raise the radiator temperature above the temperature of the equipment, which results in a higher heat rejecting capacity without increasing the size of the radiators. However, commercially available compressors have a high mass (40 kg for 10kW cooling capacity), cause excessive vibrations, and are intended for much lower temperatures (maximum 65°C) than what is required for the space heat pump application (100°C). Dedicated aerospace compressors have been developed with a lower mass (19 kg) and for higher temperatures, but these compressors have a lower efficiency. For this reason, a heat-pump demonstrator based on an electrically-driven, high-speed (200,000 RPM) centrifugal compressor system has been developed in a project funded by the European Space Agency (ESA). The main characteristics of the heat pump demonstrator are summarized in Table 1.

Saturation temperature in the evaporator	45°C
Saturation temperature in the condenser	100°C
Heat pump cooling capacity	5 kW
Total compressors power	<2.5 kW divided over 3 compressors in a serial configuration
Condenser capacity	7.5 kW (5 kW for heat load and 2.5 kW for compressor power)
Target COP	>2
Working fluid	Isopentane (R601a)
Internal volume of system	~3 liters total (~1 liter without the accumulator and receiver)

Table 1 Main characteristics of the heat pump demonstrator

II. Heat Pump Working Principle

A vapour compression Heat Pump consists of a compressor, a heat exchanger at the heat source (i.e. the evaporator), a heat exchanger at the heat sink (i.e. the condenser), and an expansion valve (see Figure 1 for a schematic drawing). The fluid enters the compressor as vapour (1). The compressor increases the pressure and the temperature of the vapour. The vapour (2) then travels through the condenser, where the vapour is condensed into liquid and the heat that is stored in the vapour is released. The liquid (3) flows through the expansion valve, where the pressure decreases (adiabatic expansion), causing a partial evaporation of the liquid and a drop in the temperature. The cold liquid-vapour mixture (4) then flows through the evaporator where it absorbs heat and completely turns into vapour (1) before entering the compressor again. The heat pump cycle with isopentane (R601a) as working fluid and where the saturation temperature is increased from 45 to 100°C is represented in the enthalpy-pressure diagram in Figure 2. In the ideal cycle (dashed line), the fluid leaves the evaporator and enters the compressor as saturated vapour. In an actual vapour compression cycle (solid line), the vapour is slightly superheated (to 50°C) to ensure that the fluid is completely vaporized before it enters the compressor. In the ideal cycle, the compression process is isentropic, whereas in an actual cycle, the adiabatic efficiency of the compression process is approximately 60%. Furthermore, there is a pressure drop (which is assumed to be 0.4 bar) in the condenser, evaporator and transport lines of an actual heat pump. All these differences between the ideal and actual cycle have a large influence on the performance of the system, and must be taken into account in the analysis, e.g. for the fluid selection (see next chapter).

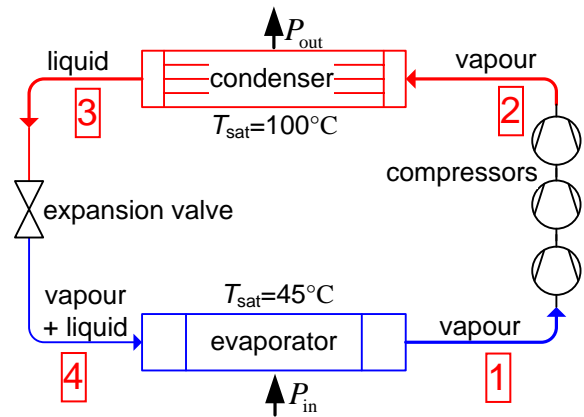


Figure 1 Schematic drawing of a heat pump

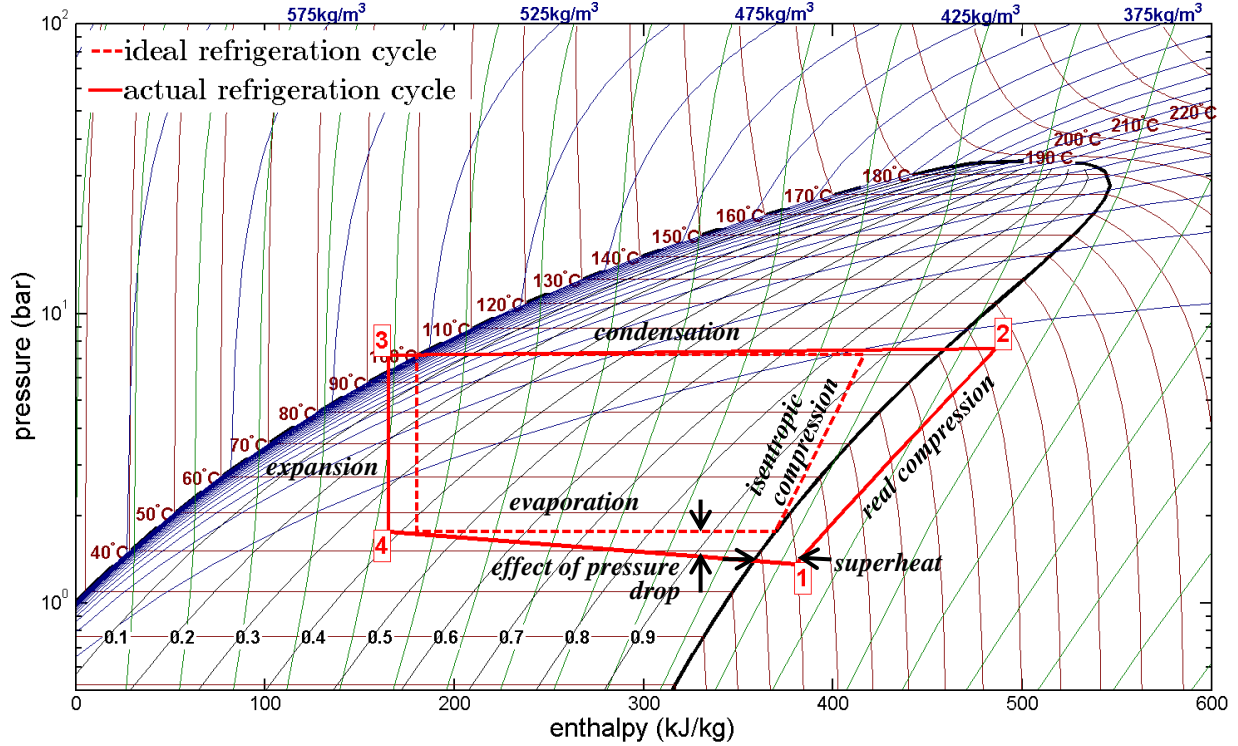


Figure 2 Pressure-Enthalpy diagram of a vapor compression cycle with isopentane (R601a) as refrigerant. The red numbers 1 to 4 correspond to the locations in Figure 1. The ‘skewed dome’ in the diagram is the two-phase region, i.e. the fluid in that region is a mixture of liquid and vapor. To the right of the dome, the fluid is vapor, to the left, the fluid is liquid. The green lines in the diagram are isentropic lines, the blue lines are isodensity lines, and the dark red lines are isothermal lines.

III. Fluid Selection

A. Selection on high COP

A very important characteristic of a heat pump for a space application is that it has a high Coefficient Of Performance (COP). The COP of a heat pump is the cooling capacity of the heat pump P_{cool} , divided by the power required for the compressor $W_{compressor}$:

$$COP = \frac{P_{cool}}{W_{compressor}} \approx \frac{h_1 - h_4}{h_2 - h_1} \quad (1)$$

where the enthalpies h with subscripts 1 to 4 refer to the enthalpies at location 1 to 4 in Figure 2. In order to find the most suitable fluid for the heat pump, the COP is calculated for a heat pump cycle for all the fluids in the REFPROP database.¹ In the calculation, it is assumed that the compressor efficiency is 60%, and the pressure drop over the evaporator and condenser is 0.4 bar. Furthermore, the fluid must have a compressor outlet pressure below 14 bar, because with higher pressures the gas friction losses increase and the compressor internal

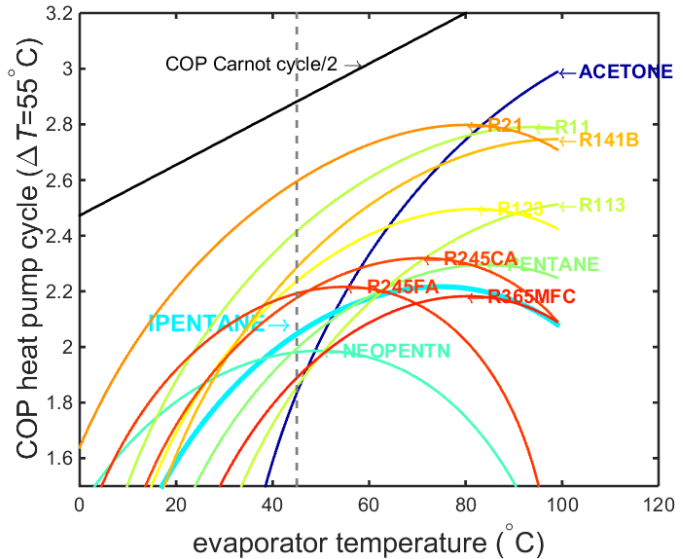


Figure 3 Calculated COP for a heat pump with different fluids. The lines are colored according to the alphabetical order of the names of the fluids

temperature limits would be exceeded. Figure 3 shows the

calculated COP for a heat pump cycle for which the temperature difference between the evaporator and condenser is 55°C (Ref. 2). According to this figure, the most suitable fluids for the heat pump with an evaporator temperature of 45°C are R21, R11, R141b, and R123. However, these fluids are banned or being phased-out according to the Montreal protocol (because of their ozone depletion potential). The next best fluids are R245fa, R245ca, and isopentane (R601a). A detailed analysis of the compressor performance showed that the efficiency of the compressor is higher for isopentane than for the R245 refrigerants, so isopentane was selected for the heat pump application. The flammability of isopentane can be suppressed by blending with 30% molar concentration of R245fa.³

B. Radiation Hardness of isopentane

In a space application, the fluid in the heat pump is exposed to radiation. The total ionizing dose is the amount of energy per unit mass transferred by particles to a target material. The total ionizing dose that is absorbed by the fluid over a 15 years GEO mission is calculated to be 16.6 kGy.

1. Type of ionizing radiation

In space, the ionizing radiation consists mainly of highly energetic protons and helium nuclei. The energy distribution of these charged particles has a peak between 100 MeV and 1 GeV, which is far more than for protons and helium nuclei (alpha particles) that are produced by radioactive decay. For example, alpha particles that are produced by alpha radioactive decay have an energy of just 5 MeV and can be blocked by a piece of paper, whereas cosmic alpha particles can penetrate a few cm of aluminium. For this reason (and for others), it is not convenient to carry out tests with alpha particles from a nuclear source. A particle accelerator is (easily) capable of accelerating protons to such high energies, but particle accelerators are not readily available for fluid sample testing. Instead, most tests in literature are carried out with gamma radiation. Although gamma radiation is completely different from high velocity protons and alpha particles, the effect of an equal ionizing dose is similar (see Appendix 2.3 in Ref. 4).

2. Substances formed due to radiation

In Ref. 5, liquid isopentane was irradiated at room temperature with a ⁶⁰Co gamma source with a total absorbed dose of 6e19 eV/g, which is equivalent to 10 kGy. The second column in Table 2 shows the yields (*G*-values) that were obtained in Ref. 5. The unit for *G* in this reference is molecules per 100eV absorbed energy. The SI unit of yield is mole/J and values in this unit can be obtained by multiplying with 1.036e-7. Column three in Table 2 shows the amount of substances that are formed with a radiation dose of 16.6 kGy. The long carbon chains (e.g. C₈ and C₁₀ in Table 2) that are formed due to radiation can form deposits on the tubing and influence the viscosity of the liquid. However, the amounts of these substances are so small, that the effect is negligible. The mass fraction of non-condensable gasses (e.g. H₂ and CH₄) that are formed due to radiation is also small. However, since the density of the non-condensable gasses is low, they could form a significant gas volume in the system. For example, the density of hydrogen is 0.13 kg/m³ at 45°C and 1.76 bar (which are the conditions in the evaporator). This means that due to the radiolysis, 0.05 litre of helium gas would form in 1 litre of liquid isopentane when the hydrogen would not dissolve in the isopentane. This amount of hydrogen is not problematic for the functioning of the heat pump. Part of the hydrogen will dissolve in the isopentane, but the solvability of hydrogen in isopentane could not be found in literature. However, information from literature on the solvability of hydrogen in larger alkanes⁶, in alcohols^{7,8} and the similar solvability of nitrogen in pentane and larger alkanes⁹, seem to suggest that all the formed hydrogen will be dissolved in the isopentane.

In order to investigate the influence of temperature, radiation dose, and type of radiation, papers on the radiolysis of n-pentane¹⁰⁻¹² were studied. In Ref. 10, liquid n-pentane was irradiated with different doses with a ⁶⁰Co gamma source and at different temperatures (between -196°C and 100°C). The test results show that there is some dependence of yield *G* on the temperature, but the effect is relative small. In Ref. 10, the obtained yield with a ⁶⁰Co gamma source was also compared to data obtained in other experiments with ⁶⁰Co gamma sources¹², and with other types of irradiation, such as irradiation with a 2 MeV electron beam¹¹ and X-rays. From these test results, it can be concluded that the yield *G* for n-pentane is almost independent on the type of radiation and the radiation dose. It can also be concluded that the obtained yields for n-pentane and isopentane are similar. Because of the similarity between isopentane and n-pentane, it is assumed that the yields in Table 2 are almost independent of temperature, radiation dose, and type of radiation.

For comparison, the yield *G* for H₂ that is obtained by gamma radiolysis of ammonia is typically 1 (Ref. 13-14) which is 3.5 times smaller than for isopentane

3. Conclusions for the radiation hardness of isopentane

Due to the exposure of isopentane to radiation in a space application, other substances will form. However, the amounts of the formed substances are so small, that no significant influence on the performance of the heat pump is expected.

substance	Yield G (molecules/100eV)	mass fraction after 16.6 kGy dose ($\text{mass}_{\text{substance}}/\text{mass}_{\text{C}_5\text{H}_{12}}$)
H ₂	3.5	1.2e-5
CH ₄	1	2.8e-5
C ₂ H ₄	0.3	1.5e-5
C ₂ H ₆	1	5.2e-5
C ₃ H ₆	0.8	5.8e-5
C ₃ H ₈	0.6	4.5e-5
C ₈	1	20e-5
C ₁₀	1	24e-5

Table 2 Radiolysis product of isopentane. The second column shows the yields obtained in Ref. 5. Column 3 shows the calculated product mass with a radiation dose of 16.6 kGy

IV. Preliminary heat pump design for a GEO satellite

A. General layout

The cooling demand for GEO communication satellites is steadily increasing. Current European-built satellites use body-fixed North/South radiators to dissipate heat. However, these body-fixed radiators can only dissipate a limited amount of energy and are at the limit of their capacity for current high-power communication satellites. A heat pump provides the opportunity to use East/West radiators. These are normally not so effective because of the higher sun inclination angle for East/West radiators (maximum inclination angle of 67°), but become very effective when the radiator temperature is elevated to 100°C.

This chapter describes a heat pump with East/West radiators as an ‘add-on’ system to a traditional GEO satellite. The North/South radiators of this satellite have a temperature of 45°C with transponders mounted directly at the backside of the radiator panels. The total effective heat dissipation capacity of the North/South radiators is 10 kW. A heat pump is used to raise the temperature of additional East/West radiators to 100°C. These radiators have a surface area of 5 m² each, which is sufficient for an additional payload heat dissipation capacity of 5 kW. The payloads (e.g. transponders) are not directly mounted on backside of the radiator panels. Instead, the payload can be located anywhere in the spacecraft, and the heat pump transports the heat from the payload to the East/West radiators.

Figure 4 shows a schematic drawing of a 5 kW add-on heat pump system with East/West radiators on a GEO satellite. Two meandering evaporator tubes are routed along the heat sources on two payload panels. The vapour from the two evaporator tubes is combined and fed into the compressor which increases the saturation temperature of the vapour from 45°C to 100°C. The vapour then travels through parallel condenser tubes, where the vapour is condensed into liquid and the released latent heat is radiated into space. The liquid is divided over two expansion valves, one for each evaporation tube, where the pressure abruptly decreases, causing a drop in the temperature from 100°C to 45°C. The two evaporator tubes are placed in a parallel configuration in order to limit the pressure drop over the tubes. Each expansion valve is controlled by the superheat temperature at the exit of its evaporator tube. This ensures that each payload platform receives the correct amount of fluid, even when the heat input from one platform is higher than from the other.

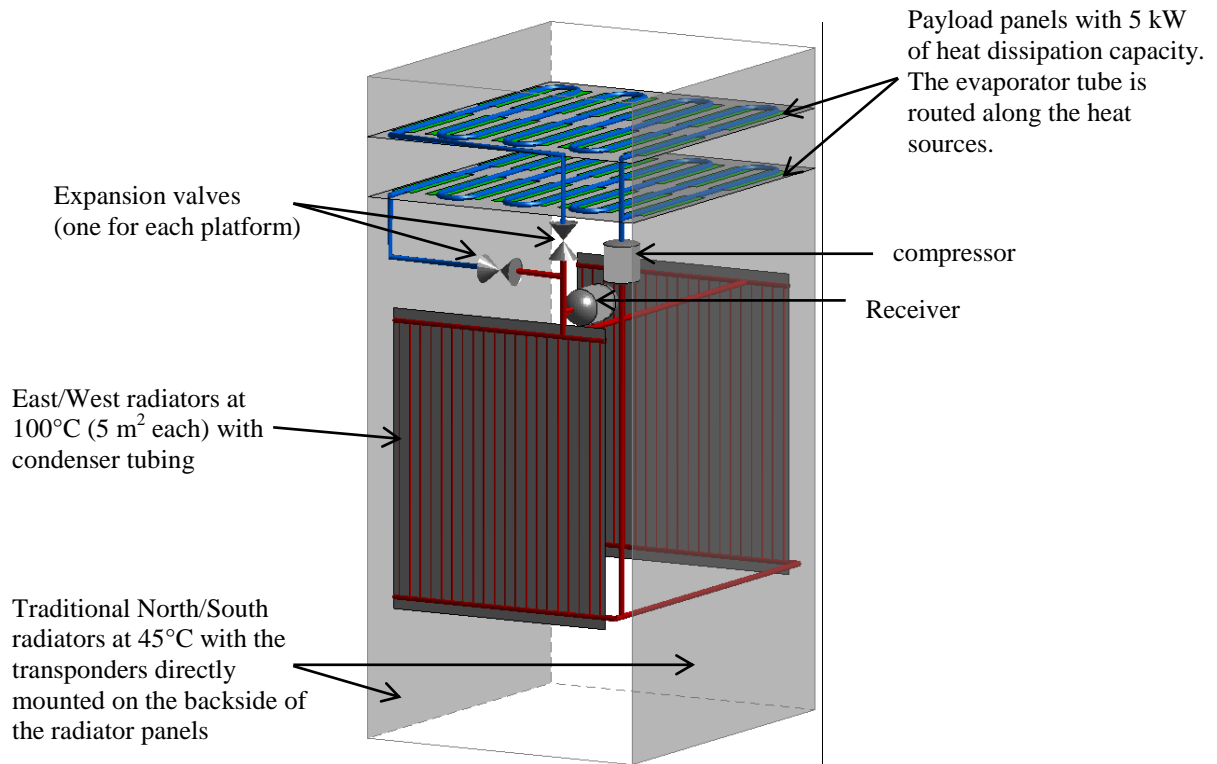


Figure 4 Schematic drawing of a 5 kW add-on heat pump system on a GEO satellite. The heat pump rejects heat via the East/West radiators.

B. Tubing diameter and pressure drop

The pressure drop in the system is calculated with the Colebrook and Muller-Steinhagen and Heck correlations. The length of each evaporator tube is 22 m. The inner diameter is 12 mm. The massflow per evaporator tube is 11.6 g/s. The pressure drop over the evaporator tube is then 0.39 bar. Note that if a single evaporator (with a length of 44 m) instead of two parallel evaporator would be used, the massflow through that single evaporator would be 23.2 g/s, and the pressure drop would be 2.8 bar.

For the condenser in the radiator, 40 parallel tubes with diameter of 1.5 mm are used in each radiator, so the spacing between the tubes is 5 cm. The length of each tube is 2.5 m. The pressure drop over the condenser is 0.27 bar. Approximately the same pressure drop would be obtained with 10 parallel tubes with a diameter of 2.5 mm, but the temperature gradient over the radiator facesheet would become very large with such a large spacing (20 cm) between the condenser tubes (see next section).

C. Temperature gradient over the radiator facesheet

A typical radiator panel consists of a honeycomb core with aluminium facesheets on both sides. Heat pipes are mounted on or embedded in the radiator panel at regular intervals (typically between 10 and 30 cm). A small interval between the heat pipes results in a small temperature gradient over the radiator, but in a high mass of the radiator. The aluminium facesheets provide stiffness to the panel, and spread the heat over the panel. A facesheet typically has a thickness between 0.2 and 0.6 mm. A thicker facesheet is a more effective heat spreader and therefore reduces the temperature gradient over the radiator. However, a thicker facesheet also results in a higher mass of the radiator. For a traditional North/South radiator panel with an effective temperature of 45°C, around 400W/m² is radiated into space. The heat pump radiators have a much higher temperature and radiate 750 W/m² into space. This higher heatflux results in a higher temperature gradient over the radiator panels. For example, Figure 5 shows the facesheet temperature as a function of the distance from a condenser tube for a heat pump radiator. In this calculation, the spacing between the condenser tubes is 20 cm (which is a typical spacing for traditional radiator panels). For a facesheet thickness of $t=0.2$ mm, the temperature of the condenser tube has to be 150°C in order to radiate 750 W/m² into space. Even for a facesheet thickness of $t=1.0$ mm, the temperature of the condenser tube still has to be 110°C. Fortunately, the condenser tubes in a heat pump application have a lower mass than heat pipes, and the spacing can therefore be smaller. For example, Figure 6 shows the facesheet temperature for a condenser tubes

spacing of 5 cm. For this spacing, the temperature gradient over the facesheet is small, even with a facesheet thickness of just 0.2 mm.

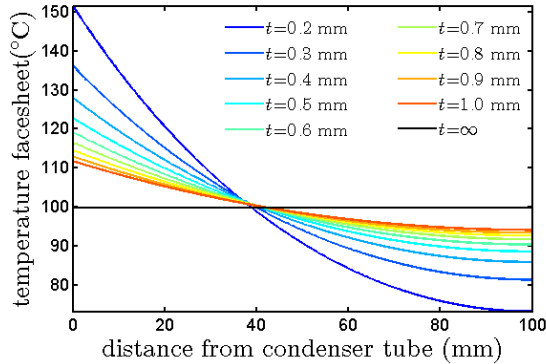


Figure 5 Temperature over the radiator facesheet with 20 cm spacing between the condenser tubes

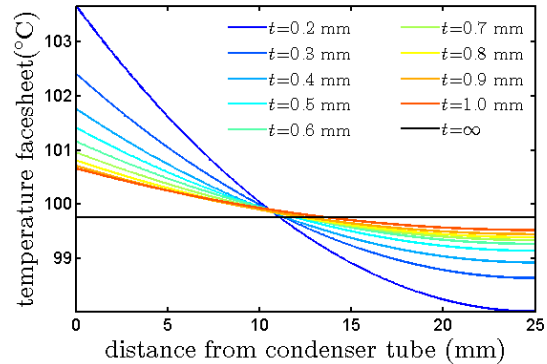


Figure 6 Temperature over the radiator facesheet with 5 cm spacing between the condenser tubes

D. Mass estimation

1. Fluid

The volume of the evaporators (2x22 m tube with 12 mm inner diameter) is 5 litres. The volume of the condensers is 0.5 litres. It is assumed that the tubing between the evaporators and condensers and the manifold tubing for the condensers is 25 m long and has an inner diameter of 15 mm. The volume of this tubing is 4.4 litres. The total liquid volume of the system is approximately 10 litres. The fluid in the system has a mass of approximately 6 kg.

2. Compressor, valves, and receiver

The compressor system has a mass of approximately 2 kg. The electronics for the compressor is assumed to be 4 kg. The valves have a mass of 1 kg. The receiver (which is a liquid storage vessel in the heat pump) is assumed to have a mass of 4 kg.

3. Tubing

For the tubing, a wall thickness of 1 mm is assumed. According to chemical compatibility guides, the compatibility of aluminium and pentane (information for isopentane is not available) is excellent. It is therefore assumed that the tubing is made of aluminium. The total mass of the tubing is then 7.7 kg.

4. Radiators

The mass of a traditional radiator panel depends on the thickness of the facesheet, the density of the honeycomb core, and the spacing between the heat pipes. A traditional radiator panel has a mass of approximately 6.6 kg/m² (see Table 3 for the mass division over the different components). A heat pump panel can be made lighter, because the condenser tubes have a lower mass than the heat pipes that are used in traditional radiator panels. The spacing between the tubing can therefore be made smaller, which results in a thinner required facesheet thickness. Furthermore, a traditional radiator panel has the payload directly attached to it, and therefore has to be stronger and stiffer than a heat pump radiator panel. For this reason, the honeycomb core can be lighter.

The condenser tubes have an inner diameter of 1.5 mm, and a wall thickness of 1 mm. They can be connected to the facesheet with a flange of 2 mm thick and 5 mm wide. The total mass of a heat pump radiator panel is 3.3 kg/m² (see Table 3). Since the total surface area of the heatpump radiators panel is 10 m², the total mass of the radiators is 33 kg.

	Mass of traditional radiator panel (kg/m ²)	Mass of Heat pump panel (kg/m ²)
OSR incl. adhesive	0.48	0.48
2x aluminium facesheet	1.6 (0.3 mm thick)	1.1 (0.2 mm thick)
Honeycomb core	1.75 (25 mm, $\rho=70$ kg/m ³)	0.88 (25 mm, $\rho=35$ kg/m ³)
Heat pipe or condenser tube	2.8 (heat pipe every 15 cm)	0.83 kg (tube every 5 cm)
Total	6.6	3.3

Table 3 Mass estimation for a traditional and a heat pump radiator panel

5. Mass penalty for electric power usage

The compressor of a heat pump system with a COP of 2 and a cooling capacity of 5 kW has a power consumption of 2.5 kW. This power consumption results in a higher mass of the spacecraft due to larger solar panels and batteries. This extra mass is approximately 25 kg/kW (Ref. 16). The total mass penalty for the electrical power usage is then 62.5 kg.

6. Mass penalty for redundancy

A puncture or a leak in the system represents a single point failure. This single-point failure can be prevented by adding an extra redundant heat pump system. This doubles the mass for the tubing, compressor, receiver, valves, and fluid. The redundant system can share the same radiator panel with the main system, so the mass of the radiators is not doubled, but only increased with 8.3 kg (for the additional condenser tubes).

Since the compressors have a relative low mass, they can also be made redundant without a large mass penalty. For this reason, it is assumed that both the main and the redundant heat pump loop have an additional compressor system (so four compressor systems in total).

7. Mass summary

A summary of all the masses in a heat pump system is provided in Table 4. The basic system has a mass of 120 kg. The system with an additional redundant heat pump system and additional compressor systems (so four compressor systems in total) has a mass of 165 kg.

	Mass of a basic 5 kW heat pump system (kg)	Mass of 5 kW Heat pump system with redundancy (kg)
Fluid	6	12
Compressors, valves, receiver	11	34
Tubing	7.7	15.4
Radiators	33	41
Electric power usage	62.5	62.5
Total	120.2	164.9

Table 4 Mass estimation for a basic and redundant heat pump system

8. Micrometeorites and space debris

In order to be less vulnerable to impacts of micrometeorites and space debris, the radiators could be equipped with heat pipes instead of condenser tubes. The heat then has to be conducted from a condenser section to the heat pipes that are attached to the radiator. However, this solution results in a large mass increase of the system, since a radiator with heat pipes has a larger mass than a radiator with condenser tubes (see Table 3). Furthermore, the thermal performance of such a system is worse, because of the additional temperature gradient between the condenser section and the heat pipes, and the lower thermal performance of a radiator panel with relative large spacing between the heat pipes (compare Figure 5 with Figure 6).

V. Heat Pump Demonstrator

A. General layout

A heat pump demonstrator with the three novel electrically-driven high-speed centrifugal compressors in a serial configuration has been designed and built. The objective of the demonstrator is to investigate the efficiency of the compressors, the COP of the overall system, and to identify issues with e.g. start-up or oscillations between the three serial compressors. Figure 7 shows a CAD drawing of the heat pump demonstrator, whereas Figure 8 shows an actual picture of the hardware. At the inlet and outlet of each compressor, the pressure and temperature is measured, so that the isentropic efficiency of each individual compressor can be calculated, as well as the efficiency of the total compressor system. The 5 kW heat load in the evaporator is applied by running 'hot' water (e.g. 60°C, which is supplied by a thermostat bath) through a commercial plate heat exchanger (SWEP B10T14). A similar plate heat exchanger (SWEP B8TH20) is also used for the condenser. An electronic expansion valve (Danfoss-Saginomiya VKV-20D32) is used to control the vapour superheat temperature.

The massflow is measured with a Bronkhorst M55 coriolis flow meter. The pressure is measured with GE sensing A50D6-TB-A1-CC-HO-PS pressure sensors. The accuracy of the pressure sensors is ± 0.068 bar ($\pm 0.34\%$ full range). The temperature sensors are standard thermocouples which have an accuracy of 0.5°C with the data acquisition card that is used. The data acquisition system is a National Instruments CompactRIO system in combination with LabVIEW software. The software displays the vapour compression cycle in the pressure-enthalpy

diagram in real time, which is very important since it must be prevented that the high-speed centrifugal compressors ingest liquid refrigerant during operation. The motors of the compressors are cooled by cooling water. The massflow and temperatures of this cooling water is measured, such that the amount of energy that is removed from each compressor by the cooling water can be calculated. In a next stage of the project, the motors of the compressors will be cooled by the refrigerant itself (i.e. by isopentane from a bypass directly after the expansion valve). The compressors are discussed in more detail in the next section.

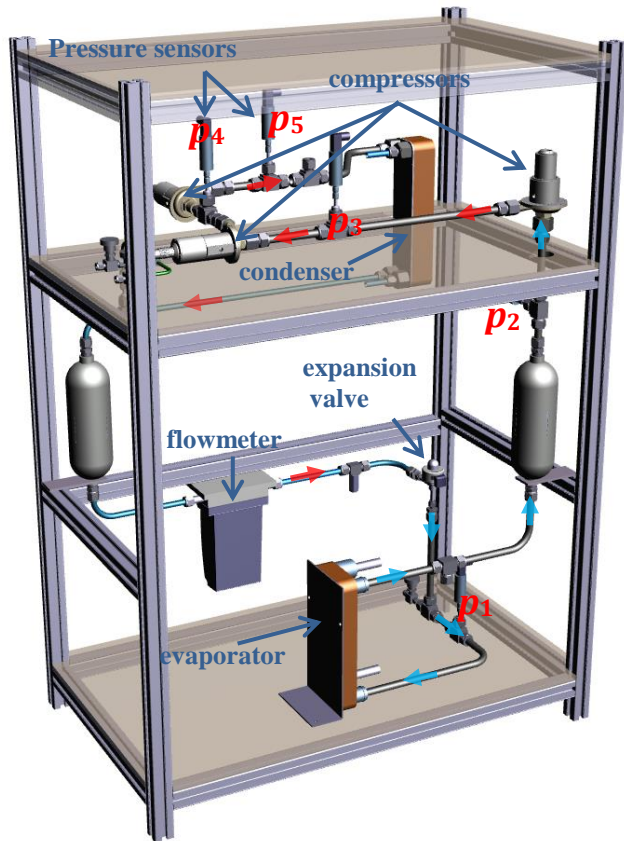


Figure 7 CAD drawing of the heat pump. The small red and light-blue arrows indicate the direction of the flow. The locations of the 5 pressure sensors are indicated with p_1 to p_5

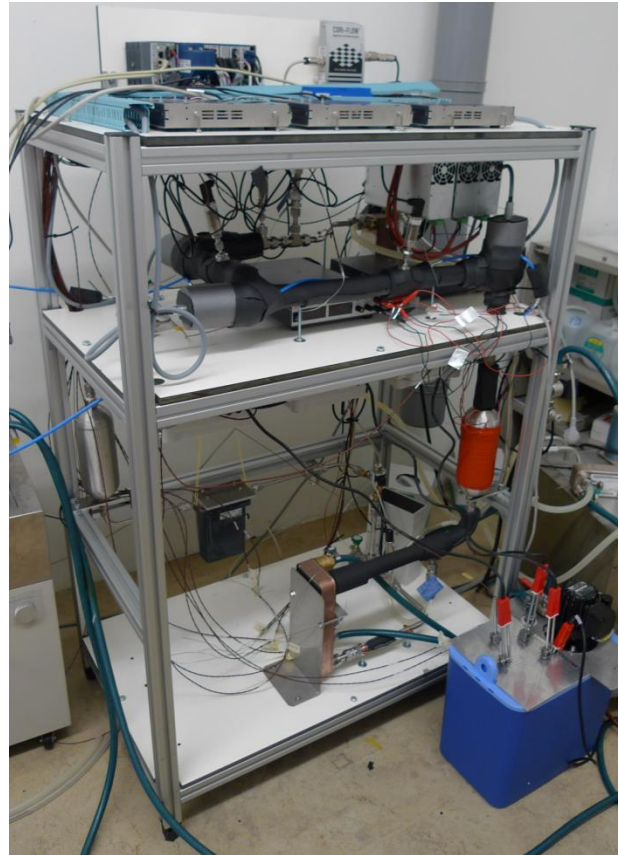


Figure 8 Photo of the demonstrator

B. Compressors

Three electrical-driven turbo compressors made by Celeroton are used in a serial configuration. For the first stage, a (slightly modified) existing CT-17-700 turbo compressor with a 3D impeller with a diameter of 21 mm has been used¹⁷. For the second and third stage, a new turbo compressor with a 2D impeller with a diameter of 23 mm has been designed¹⁸ as part of this project. Figure 9 shows a CAD drawing of the second stage compressor, whereas Figure 10 shows a photo of the impeller. The compressors run approximately at 180,000 RPM. The compressors are equipped with ball bearings, and the lifetime of these bearings is not yet sufficient for space missions. In a next stage of the project, bearings with a longer lifetime will be used.

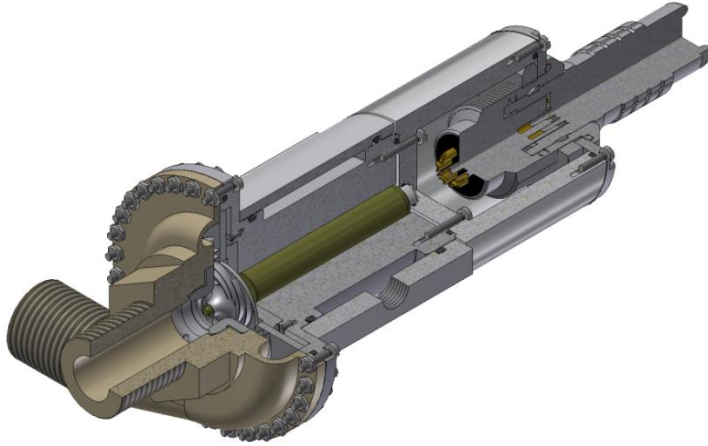


Figure 9 CAD drawing of the 2nd stage compressor



Figure 10 Rotor with a stage two impeller mounted

In Ref. 19, a comparison has been made between commercial and aerospace compressors, and the compressors developed in this project. From the comparison, it can be concluded that the compressor developed in this project have:

- A mass of 2 kg (650 g each), compared to >20 kg for other compressors with the same capacity
- A vibration level of <0.3 N compared to 40 N for commercial compressors
- An isentropic efficiency of 68%, which is higher than aerospace compressors (46%, which would result in a COP of 1.7), and comparable to commercial compressors (60-70%)
- A condenser saturation temperature of 100°C, which is comparable to aerospace compressors, but higher than the maximum temperature of commercial compressors (65°C)
- No oil required for lubrication or sealing, compared to commercial compressors which require a few litres of oil

C. Measurement results

Figure 11 shows the pressure during a measurement (see Figure 7 for the locations of the pressure sensors). At $t=0$, the system is at rest. Shortly after, the rotational speed of the compressors is increased in small steps and the pressure differences in the system increase. At $t=155$ minutes, a steady state is achieved at the desired cooling load and system temperatures. At this moment, the pressure ratio delivered by the compressors is 4.7 and the heat input by the evaporator into the isopentane (P_{cool}) is 5141W. The compressors deliver a hydraulic power ($W_{compressor}$) of 1445W to the fluid. The compressors are cooled with cooling water. This water removes 535W from the isopentane ($P_{cooling\ water}$) and must be taken into account in the calculation of the COP:

$$COP = \frac{P_{cool} - P_{cooling\ water}}{W_{compressor} + P_{cooling\ water}} \quad (2)$$

Figure 12 shows the measured heat pump cycle in a pressure-enthalpy diagram. At the desired temperatures and heat input, the COP is 2.3, which is higher than the requirement of 2 and better than the performance of the target cycle. This is because the pressure drop in the evaporator is lower (0.2 bar instead of 0.4 bar), and because the efficiency of the compressors is higher than was assumed in the initial calculations (68% instead of 60%). Note that the enthalpy between the compressors inlet and outlet is parallel to the isentropic lines (the green lines in Figure 12), which seem to suggest a 100% isentropic efficiency of the compressors. However, this effect is caused by the removal of heat by the compressor cooling water. When the heat removal by the cooling water is included in the energy balance, the total efficiency of the compressor is not 100%, but 68%.

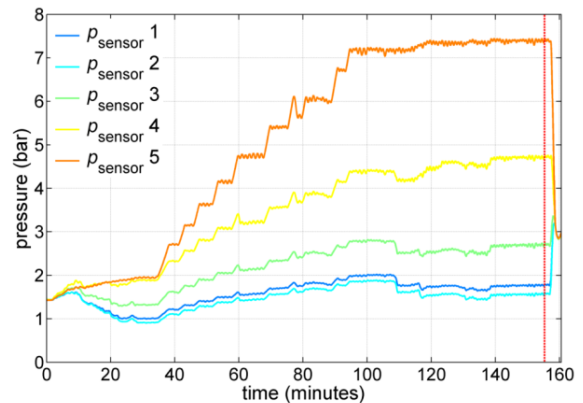


Figure 11 Measured pressures. The locations of the 5 pressure sensors are indicated with p_1 to p_5 in Figure 7

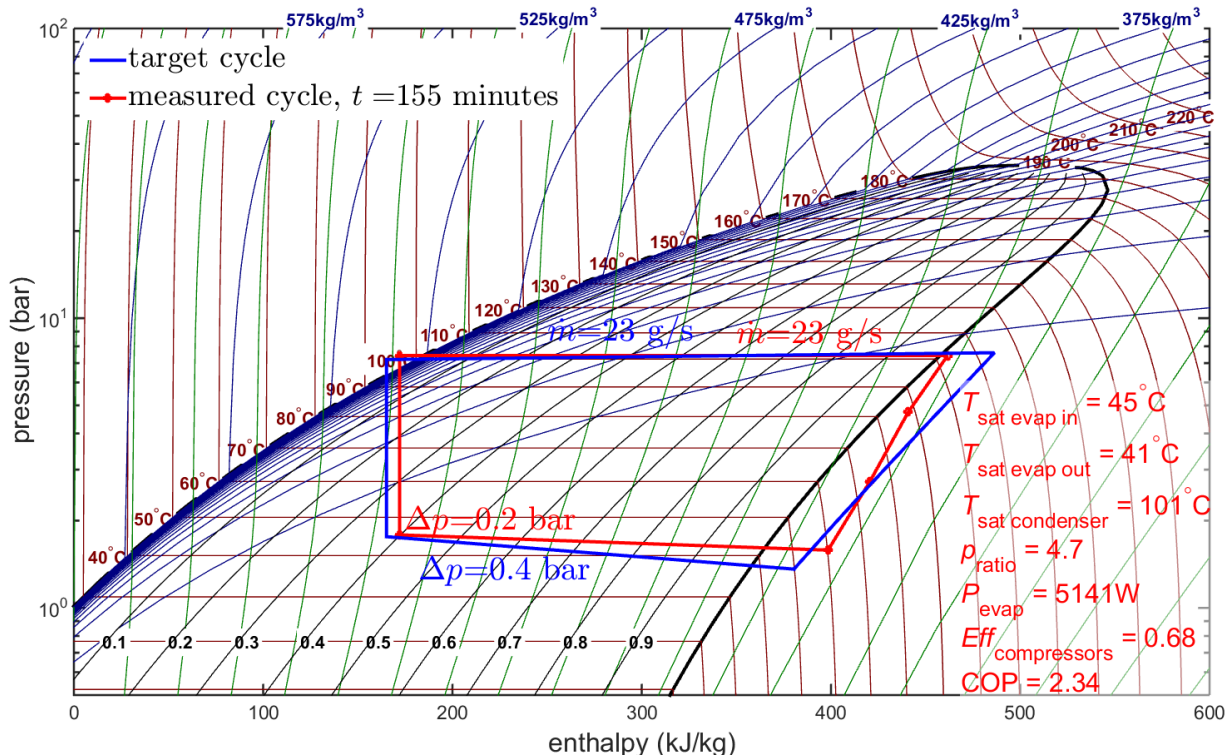


Figure 12 Measured (red) and target (blue) heat pump cycle in a pressure-enthalpy diagram. The measured cycle has a COP of 2.3, which is higher than the requirement of 2

VI. Conclusion

In this paper, a heat pump demonstrator with three novel electrically-driven high-speed compressors in a serial configuration is discussed. The work described in this paper was funded by ESA and has been carried out together with the Swiss company Celeroton. The refrigerant for the demonstrator is isopentane (R601a). It is demonstrated that the used heat pump method is very efficient: At the target setting (saturation temperature of 45°C at the evaporator, 100°C at the condenser, and a ‘payload’ heat input of 5 kW), the measured COP is 2.3, which is higher than the requirement of 2. Furthermore, the demonstrator shows that the concept with three compressors in a serial configuration is feasible (e.g. no oscillations between the three serial compressors have been observed).

The compressors developed in this project have a much lower mass and higher efficiency than existing (commercial or aerospace) compressors.

The compressors for this project phase have been equipped with ball bearings, as the goal of this project was to prove the thermodynamic feasibility of the concept. Therefore, the lifetime is not yet sufficient for space missions. The main focus of the current research is into increasing the lifetime of the bearings e.g. by using contactless bearings. Further work includes space qualifying the compressor electronics, cooling of the compressor with the refrigerant fluid, and designing a receiver that works in zero gravity. Furthermore, the use of a Liquid Suction Heat Exchanger (LSHE, see Appendix) is investigated, since this can increase the COP of the total system, and inherently provides the required superheating of the vapour before it enters the compressors.

Appendix: A Liquid Suction Heat Exchanger (LSHE)

For a ‘wet’ refrigerant like isopentane, the two-phase dome is ‘tilted’ to the right. As a result, the liquid/vapour mixture that enters the evaporator has a relative high vapour mass fraction of 0.38. This means that 38% of the latent heat of the fluid is not used in the evaporator. A Liquid-Suction Heat Exchanger (LSHE) uses the cold vapour coming from the evaporator to cool the hot liquid from the condenser (see Figure 13). When the liquid coming out of the condenser is cooled to 60°C, the vapour mass fraction of the liquid/vapour mixture that enters the evaporator is reduced to 0.11 (see Figure 14). As a result, extra cooling capacity is achieved with almost the same compressor power, and this increases the COP from 2.6 to 3.1. Furthermore, the LSHE provides the required superheating of the vapour before it enters the compressors. The drawbacks of a LSHE are the additional mass of the heat exchanger, and the additional pressure drop in the heat exchanger.

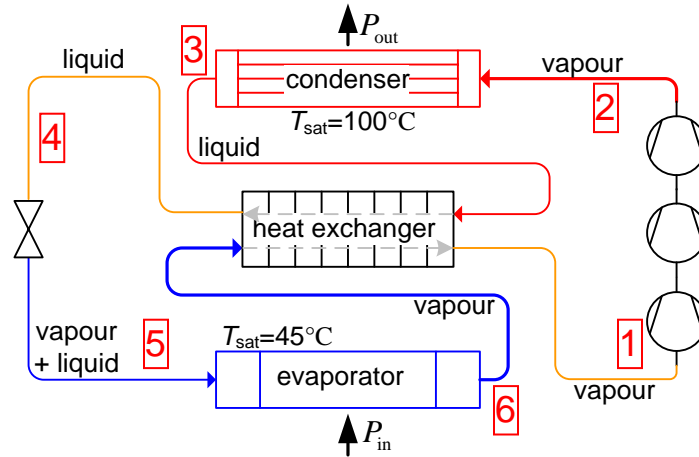


Figure 13 Schematic drawing of a vapour compression cycle with a Liquid Suction Heat Exchanger

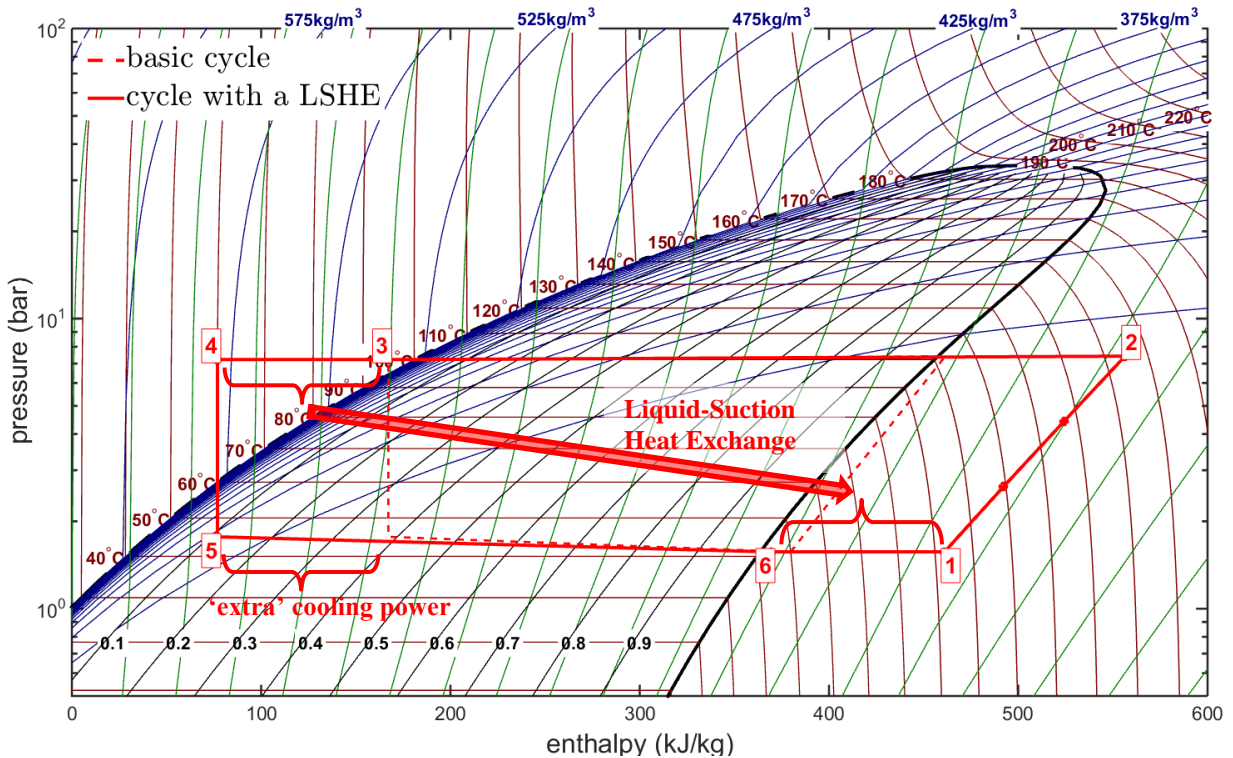


Figure 14 Vapour compression cycle with a Liquid-Suction Heat Exchanger

References

- ¹Lemmon, E.W., Huber, M.L., McLinden, M.O. "NIST Standard Reference Database 23: Reference Fluid Thermodynamic and Transport Properties-REFPROP", Version 9.1, National Institute of Standards and Technology, Standard Reference Data Program, Gaithersburg, 2013
- ²van Gerner, H. J., van Benthem, R. C., van Es, J., Schwaller, D., Lapensée, S., "Fluid selection for space thermal control systems", 44th International Conference on Environmental Systems, ICES-2014-136
- ³Garg, P., Kumar, P., Srinivasan, K., Dutta, P., Evaluation of isopentane, "R245fa and their mixtures as working fluids for organic Rankine cycles", *Applied Thermal Engineering* 51, 292-300 (2013).
- ⁴Fortescue, P., Stark, J., *Spacecraft systems engineering*, ISBN 0471927945, John Wiley & Sons, 1992
- ⁵Bryl-Sandelewska, T., Broszkiewicz, R.K., "γ-radiolysis of liquid pentanes. The role of positive ions in the formation of stable products in irradiated isopentane and n-pentane", *Radiation Physics and Chemistry*, Volume 10, Issues 5–6, Pages 309-314 (1977)
- ⁶L. J. Florusse, L.J., Peters, C.J. Pàmies, J.C., Vega, L.F, and Meijer, H. "Solubility of hydrogen in heavy n-alkanes: Experiments and soft modelling", *AIChE Journal* Volume 49, Issue 12, pages 3260–3269 (2003)
- ⁷Descamps, C., Coquelet, C., Bouallou, C., Richon, D., "Solubility of hydrogen in methanol at temperatures from 248.41 to 308.20K", *Thermochimica Acta*, Volume 430, Issues 1–2, Pages 1-7 (2005)
- ⁸Brunner, E., "Solubility of Hydrogen in Alcohols, *Berichte der Bunsengesellschaft für physikalische Chemie*", Volume 83, Issue 7, pages 715–721 (1979)
- ⁹Battino, R., Rettich, T.R., and Tominaga, T., "The Solubility of Nitrogen and Air in Liquids", *J. Phys. Chem. Ref. Data* 13, 563 (1984)
- ¹⁰Koch, R.O., Houtman, J.P.W., Cramer, W.A., "The Radiolysis of Liquid N-pentane", *J. Am. Chem. Soc.*, 90 (13), pp 3326–3333 (1968)
- ¹¹De Vries, A.E., Allen, A.O., "Radiolysis of Liquid n-Pentane", *J. Phys. Chem.*, 63 (6), pp 879–881 (1959)
- ¹²Claes, P., Rząd, S., "Electron Irradiation of Hydrocarbons I. Radiolysis of Liquid N-Pentane", *Bull. Soc. Chim. Belges*, 73: 689–702 (1964)
- ¹³Delcourt, M.O., Belloni, J., and Saito, E., "Spectrophotometric studies of the radiolysis of liquid ammonia", *The Journal of Physical Chemistry* 80 (10), 1101-1105 (1976)
- ¹⁴Eyre, J.A., and Smithies, D., "Primary yields in the γ-radiolysis of ammonia", *Trans. Faraday Soc.*, 66, 2199-2209 (1970)
- ¹⁵Toi, Y., Peterson, D.B., and Burton, M., "Effect of Density in Radiolysis of Ammonia", *Radiation Research* Vol. 17, No. 3 pp. 399-407 (1962)
- ¹⁶Goldman, J.H., Harvey, A., Lovell, T., Walker, D.H., "Lunar base heat pump, phase 1", NASA techdoc 19950011696 (2004).
- ¹⁷Zhao, D., Krahenbuhl, D., Blunier, B., Zwysig, C., Dou, M., Miraoui, A., "Design and Control of an Ultra High Speed Turbo Compressor for the Air Management of Fuel Cell Systems", *Proc. of the Transportation Electrification Conference and Expo (ITEC 2012)*.
- ¹⁸Casey, M.V., Krahenbuhl, D., Zwysig, C., "The design of ultra-high-speed miniature centrifugal compressors," *Proc. of the European Turbomachinery Conference (ETC 2013)*.
- ¹⁹van Gerner, H.J., Heat Pump Conceptual Study and Design; Overall assessment and further work, NLR-CR-2014-009 (2014)